

## SEPARATION OF FAST NUCLEAR REACTION PRODUCTS

Peter Armbruster

Gesellschaft für Schwerionenforschung, Darmstadt, West Germany

Dedicated to Professor H. Maier-Leibnitz on his 65th birthday.

### 1. Production of nuclear reaction products

Isotopes are produced in nuclear reactions. They are borne as partly stripped and highly charged, fast and energetic particles. Methods to separate isotopes will be discussed, which make use of these gifts of nature to the newborn. Its youthful equipment may be maintained during several microseconds, a time long enough to sort out and separate nuclear reaction products directly. It will be shown, that the juvenile and wild beasts can be tamed. The time consuming processes of education, as there are slowing down, reionising and reaccelerating, the ingredients of conventional isotope separation, can be avoided. Three different experimental approaches have been successfully realized which all have in common to deliver within microseconds spatially separated beams of reaction products. The latter may be investigated or identified finally by making use of their radioactivity. All methods to be discussed deliver rates higher than  $10^4$  separated particles per second. Sophisticated decay scheme studies thus are possible within reasonable measuring times.

Setting a time limit of about 1 day to do a successful experiment at one of our expensive isotope producing nuclear facilities, the rates of separated isotopes should have minimum values for different kinds of experiments. Table 1 gives these minimum rates for different fields of applications.

Table 1: Minimum separated rates necessary for good quality work in different fields of applications.

Decay schemes by $\gamma$ -spectroscopy	> $10^4$ /sec
Main $\gamma$ - and $\alpha$ -energies Isotopic yields $W(A,Z)$	> $10^2$ /sec
Halfives from strong single lines Excitation functions	> 1/sec
New Isotopes far off stability	> $10^{-2}$ /sec
Search for strange beasts	> $10^{-4}$ /sec

To compete in spectroscopic studies rates of separated isotopes of  $10^4$ /sec should be available. The hunting of interesting rare beasts, as superheavy nuclei, still may be justified with rates of  $10^{-4}$ /sec.

The isotope producing reactions, spalla-

tion, fission or heavy ion reactions are giving different production rates. Beam intensities, target thicknesses, and cross sections vary considerably. The production of ( $10^{10}$ - $10^{11}$ ) reaction products per second is possible in spallation reactions, as well as in thermal neutron fission. The smallest reaction rates are obtained at heavy ion accelerators, as targets become thin, beam strengths restricted, and cross sections low. A few times  $10^6$ /sec in most favourable cases is the highest production rate possible. The reaction rates at modern isochronous cyclotrons are between the two extreme cases.

The high primary production rates for fission and spallation products allow the application of low efficiency separating techniques. Even an efficiency of  $10^{-7}$  still gives separated rates of  $10^4$ /sec, if the primary production rate is  $10^{11}$ /sec. Low efficiency techniques are applicable in these cases, if they offer any other compensating advantages. However, to obtain at heavy ion accelerators separated rates of  $10^4$ /sec an efficiency of the separating device of ( $10^{-2}$ - $10^{-3}$ ) is required. Only high efficiency techniques should be used at these facilities.

### 2. The Different approaches

Separation times and efficiencies which have been obtained with modern separators are compared in table 3. Existing mass separators of the second generation which will be discussed in section 3, stand for realizations of the different approaches. Separation times in the 0.1 sec- region characterize ISOL-systems, whereas times of  $10^{-6}$  sec are possible with direct techniques. The separation efficiency strongly varies from element to element for ISOL-systems, whereas no such dependence principally is to be expected for separations of fast reaction products. The efficiency of ISOL-systems may be high, whereas it is low for the direct methods. The low efficiency of the latter will be overcome in the case of favourable kinematics, as it is found in a fusion reaction. Here all advantages of the direct methods are realized without the drawback of low efficiency. The price to be paid is a restriction to one type of nuclear reaction.

To determine the mass and atomic number of an unknown isotope several measurements have to be undertaken. The steps necessary in the different approaches are presented in fig. 1. As only the direct methods are my subject, I will only comment the principle of those.

Table 2: Maximum production rates for different isotope producing nuclear reactions.

	Spallation products	Fission products ( $n_{th}, f$ )	Heavy ion reaction products
Particle rates on target (particles/sec)	$6 \cdot 10^{13}$	$(1-3) \cdot 10^{15}$	$5 \cdot 10^{12}$
Target atoms (atoms/cm <sup>2</sup> )	$4 \cdot 10^{23}$	$(1-3) \cdot 10^{18}$	$(0.3-1) \cdot 10^{19}$
Cross section (cm <sup>2</sup> )	$< 10^{-26}$	$< 10^{-23}$	$< 10^{-25}$
Max. Reaction rates (products/sec)	$2 \cdot 10^{11}$	$10^{10}-10^{11}$	$(2-5) \cdot 10^6$
Efficiency necessary to give $N > 10^4$ /sec	$5 \cdot 10^{-8}$	$10^{-6}-10^{-7}$	$(2-5) \cdot 10^{-3}$

Table 3: Main characteristics of different approaches to separate shortlived isotopes

	ISOLDE II (Genf 1975)	LOHENGRIN (Grenoble 1974)	JOSEF (Jülich 1974)	SHIP (Darmstadt 1976)
Efficiency	$(0.5-5) \cdot 10^{-1}$	$1.8 \cdot 10^{-6}$	$1.4 \cdot 10^{-4}$	$(0.5-5) \cdot 10^{-1}$
Separation time (sec)	$10^{-2}$	$2 \cdot 10^{-6}$	$10^{-6}$	$5 \cdot 10^{-7}$
Efficiency atomic number dependent	yes	no	no	no
Efficiency reaction dependent	no	no	no	yes

### 2.1 Electric and magnetic field separators

A combination of electric  $F_{pe}$ , and magnetic  $B\rho_m$  field deflections allows to measure the velocity  $v$  and charge to mass ratio  $q/A$  of a charged particle.

$$B\rho_m \sim \frac{Av}{q} \quad v \sim \frac{F_{pe}}{B\rho_m}$$

$$F_{pe} \sim \frac{Av^2}{q} \quad \frac{q}{A} \sim \frac{F_{pe}}{(B\rho_m)^2}$$

Masses may be determined, if the ionic charge

is either known or measured independently, e.g. by measuring the energy of the particles. The atomic number of the isotope has to be measured after the passage through the fields by any technique sensitive to the atomic number. Conventionally the fingerprints of radioactivity have been used. But more direct methods have become available now. The energy loss of fast heavy ions in matter differs for different atomic numbers. This difference may be used to measure the atomic number. Charges up to  $Z=50$  thus have been determined.

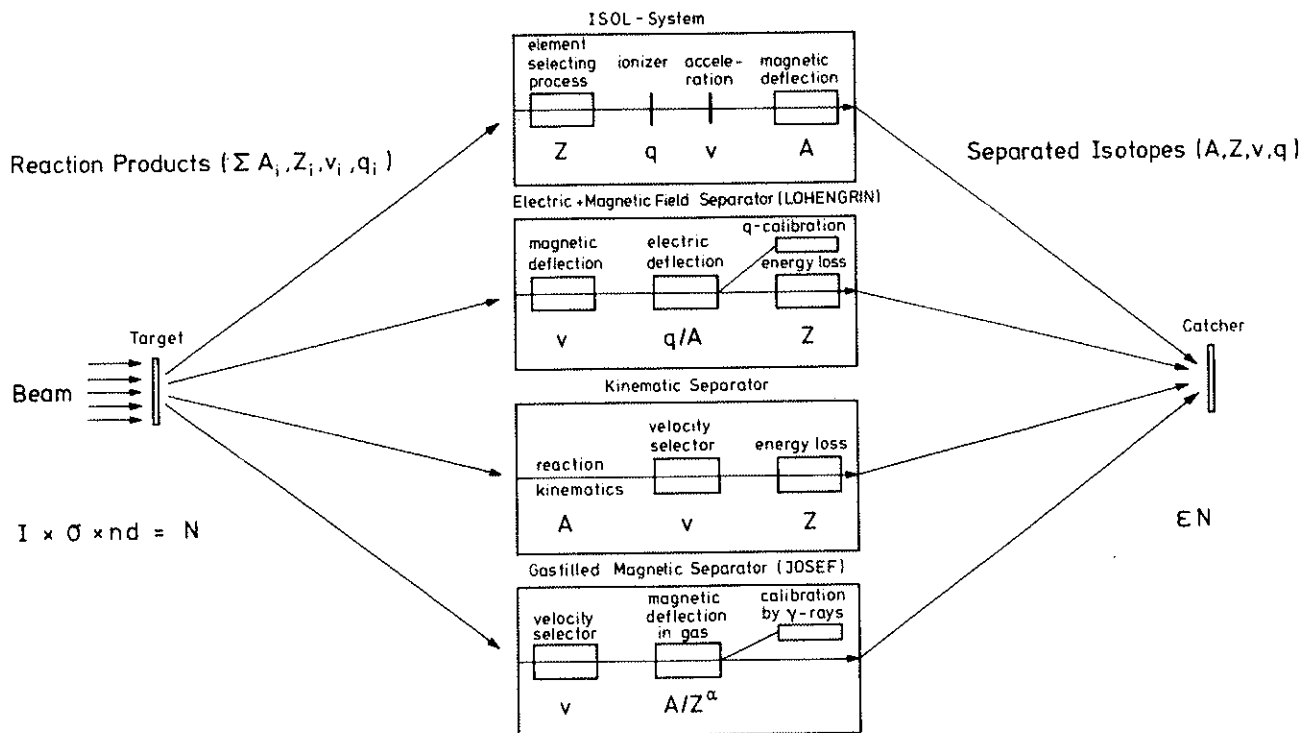


Fig. 1. Schemes of different methods to separate shortlived isotopes

The first separator applying deflection in electric and magnetic fields to fission products was a Herzog-Mattauch type of separator<sup>1)</sup>. A very similar facility is reported to be installed at a reactor in Taschkent, USSR<sup>2)</sup>. The separator LOHENGRIN installed at the high flux reactor, Grenoble is the latest member in this family<sup>3-5)</sup>. It will be discussed in section 3.1.

## 2.2 Gas-filled magnetic separators

The deflection in a magnetic field depends on the average charge of the ion during its passage through the magnetic field.

$$B\rho \sim A \frac{v}{q}$$

The ratio  $v/q$  only weakly depends on the velocity, it is mainly a function of the atomic number.

$$B\rho \sim A \cdot f(Z)$$

A large velocity window and the full ionic charge distribution is accepted giving rise to a relatively high efficiency of the method. The deflection in a gas-filled field, the gas providing the averaging over all possible ionic charges, depends on the mass and atomic number. The resolution is governed by two properties of the ion, the atomic number dispersion and the fluctuations of the average ionic charges. A gas filled separator has to be calibrated either with well defined beams of heavy ions

or with reaction products, which are known and radioactive.

Gas-filled separators have been built at various reactors<sup>6-8)</sup>, as well as at the Dubna heavy ion cyclotron<sup>9)</sup>. The only facility in operation now is the Jülich On line Separator for Fission products, JOSEF<sup>10,11)</sup>. It will be discussed in section 3.2.

## 2.3 Kinematic Separators

The conservation of mass and momentum in a fusion reaction demands that the fused product of mass A is emitted in beam direction with a well defined velocity v.

$$A = A_1 + A_2$$

$$v = \frac{A_1}{A_1 + A_2} \cdot v_1$$

$A_1$  and  $A_2$  are the masses of the projectile and the target,  $v_1$  is the velocity of the projectile hitting the target nucleus at rest. Particles of velocity v emitted in beam direction must be fusion products. A velocity filter selecting these particles is a kinematic mass separator. As projectiles and fusion products both are flying in beam direction with different velocities the separation problem is characterized by the suppression factor of primary projectiles ( $10^{13}/\text{sec}$ ) in the velocity window of the

fusion products. The number of projectiles to reaction products at the entrance to the filter is larger than  $10^8$ . Suppression factors of at least this order of magnitude have to be demanded. Near the Coulomb barrier radial and axial acceptance angles of  $3^\circ$  guarantee a transport of 70% of the evaporation residues produced after fusion through the velocity filter.

Different versions of velocity filters in connection with the problem of isotope separation have been discussed<sup>12-15</sup>). Two filters are operating. A combination of RF-electric deflection and static magnetic deflection has been built at the Tandem accelerator, Munique<sup>16</sup>). A system using static electric and magnetic fields is operating at Darmstadt<sup>17,18</sup>). This Separator for Heavy Ion reaction Products (SHIP) will be discussed in section 3.3.

#### 2.4 General Conclusions

Table 4 summarizes the maximum values of separated rates of isotopes to be expected from different isotope producing reactions and different separation techniques. From this comparison the following conclusions concerning isotope production may be drawn.

- 1) Never compete with ISOL-systems, if ISOL-systems separate the element with high efficiency and the halflife is not smaller than 0.1/sec. In this case at reactors as well as at accelerators ISOL-systems will give the highest rates.
- 2) Rates giving a chance to do high standard nuclear spectroscopy are produced at reactors using electric and magnetic field separators and gas-filled separators. At accelerators only the kinematic separators for fusion products give sufficient rates.
- 3) The direct methods are without competition from ISOL-systems
  - a) in the time window ( $10^{-1}$ - $10^{-7}$ )sec.

b) for reaction studies, e.g. yield measurements of fission fragments or evaporation residues and yield dependences from primary kinetic energies.

c) for nuclear spectroscopy of isotopes from elements, which are not separated with ISOL-techniques.

4) The draw back of the low efficiency of gas-filled separators and of electric and magnetic field separators makes their application as isotope production facilities at accelerators doubtful. For reaction studies such a system has been installed at the Brookhaven Tandem<sup>19</sup>).

5) As second stages behind kinematic separators for fusion products they may be helpful devices even for spectroscopic studies.

#### 3. The new generation of separators

The plans first discussed during the Lysekil Conference to build more powerful separators have been realized. A second generation of direct separation methods has been built during the last ten years in several European laboratories. They have been tested and have gone into scientific production. To demonstrate the power of the three different approaches already discussed, I will give the principal specifications of the three facilities, LOHENGRIN, JOSEF and the SHIP, show some results demonstrating the separation achieved, and point out one special experiment for each of the instruments showing their specific strength.

##### 3.1 LOHENGRIN

The parabola spectrometer LOHENGRIN is operating since 1974<sup>20</sup>). The main specifications are given in table 5. The spectrometer fully meets the design parameters. Fig. 2a shows a schematic sketch of the ion optics. The q/A-spectrum of the light fission

Table 4: Rates of separated isotopes for different reactions and separation methods

Rates ( $\text{sec}^{-1}$ )	ISOL-system	Electric + magnetic field separators	gasfilled magnetic separators	Kinematic separators
High energy p-accelerators (spallation)	$5(10^{10}-10^{11})$	-	-	-
High Flux Reactors ( $n_{th,f}$ )	$5(10^8-10^9)$	$5 \cdot 10^4$	$7 \cdot 10^6$	-
Heavy Ion accelerators ( $\sigma \leq 100$ mb)	$(10^5-10^6)$	2	$5 \cdot 10^2$	$5 \cdot 10^5$

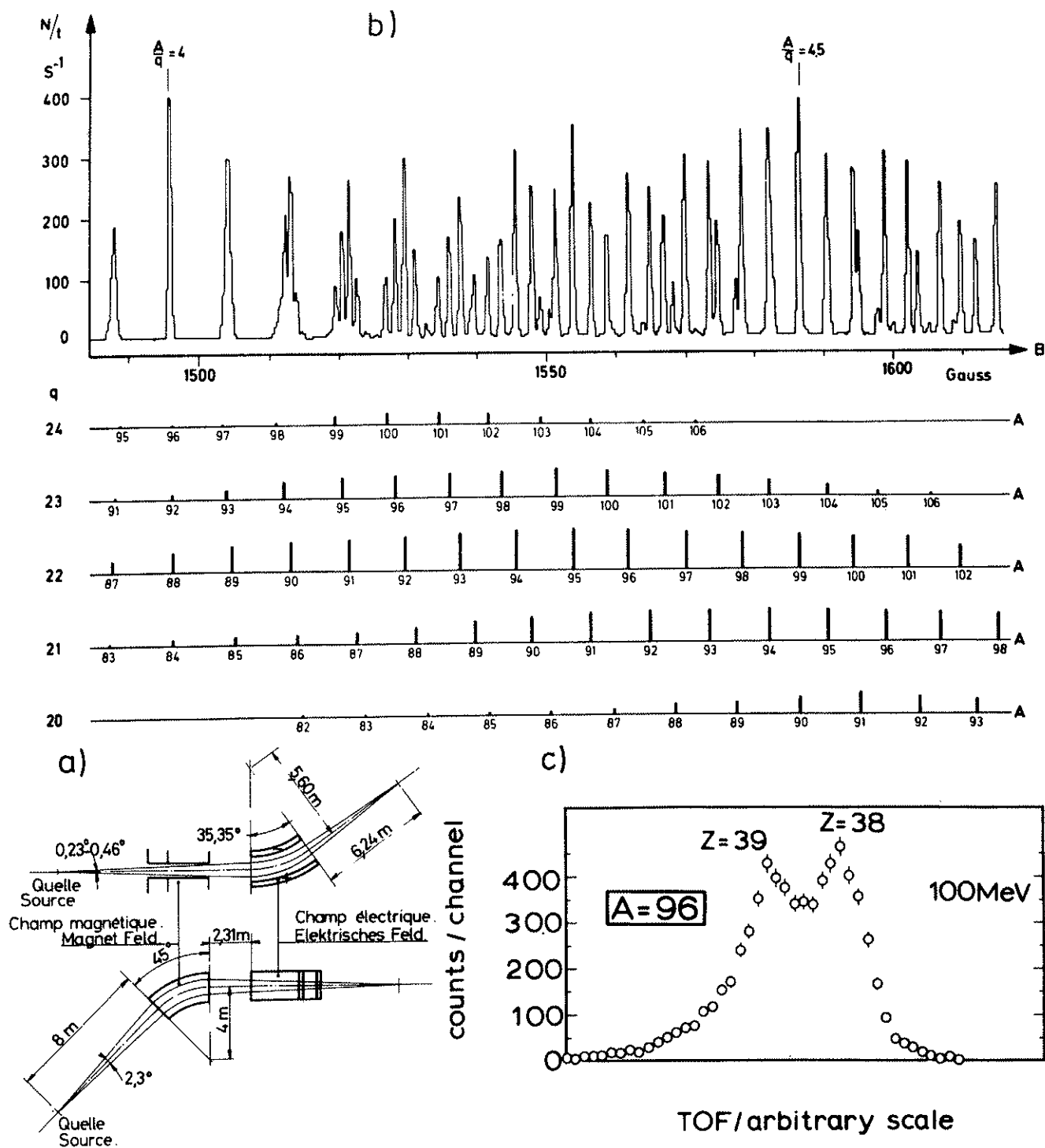


Fig. 2. a) LOHENGRIN scheme of ion optics<sup>4)</sup>.  
 b)  $q/A$ -spectrum for light fission products. The mass assignment for different ionic charges may be read from the scales given<sup>5)</sup>,  
 c) Resolved isobars of mass 96 using the energy loss-TOF technique<sup>22)</sup>.

Table 5: Specifications of LOHENGRIN

Target size (cm <sup>2</sup> )	0.3x7	0.16x4	0.01x0.5
Horizontal aperture	2.3°	2.3°	2.3°
Vertical aperture	0.43°	0.29°	0.14°
Solid angle	2.4 · 10 <sup>-5</sup>	1.6 · 10 <sup>-5</sup>	0.8 · 10 <sup>-5</sup>
Mass dispersion (m)		3.24	
Energy dispersion (m)		6.52	
Mass Resolution	800	1500	15 000 x) ≅6 MeV
Rate on 72 cm parabola (sec <sup>-1</sup> ) 400µg/cm <sup>2</sup> <sup>235</sup> UO <sub>2</sub> η <sub>AZ</sub> =2%	1.6 · 10 <sup>4</sup>	3 · 10 <sup>3</sup>	0.3 x)
Rate/parabola length (cm <sup>-1</sup> sec <sup>-1</sup> ) 40µg/cm <sup>2</sup> <sup>235</sup> UO <sub>2</sub> η <sub>A</sub> =6%	90	16	—

x) Irridiated glass detector, channel size 0.08 mm in mass direction,

product group is shown for a fixed value of the electric field as a function of the magnetic field, fig. 2b. The multiplets near full values of q/A directly give the q/A-resolution. It is larger than 800. The mass assignment is unique. It has been obtained from an analysis of the multiplet structure, from an independent energy measurement of the fission products, or from an identification of specific  $\gamma$ -transitions. The isobaric chains are resolved directly by an energy loss measurement in solid absorbers <sup>21,22</sup>). Isobars resolved in the chain A=96 are shown in fig. 2c. A time of flight technique after passage of the mass and energy defined fission products through a carbon absorber of 1.4 mg/cm<sup>2</sup> has been developed to resolve atomic numbers in the light fission product group. Absolute, isotopically resolved fission yields W(Z,A,E<sub>K</sub>) are available now for the first time <sup>23-25</sup>). In fig. 3 independent absolute yields of about 90 isotopes for two different energies are given. These measurements lead to detailed insights into the mechanisms, which govern the distribution of energy, mass, charge and angular momentum in the descent from the saddle point to scission. The last stages of fission have much in common with strongly damped collisions of two heavy ions. Their understanding may be one of the clues to understand these reactions, as heavy ion physics is far from resolving mass, charge and energy in a reaction involving about 240 nucleons. Even if the problem of resolution would have been solved principally, as in the fission case

discussed here, still the small source strength of heavy ion reactions practically would forbid a measurement of comparable quality. The most detailed experiments concerning fragmentation of nuclear matter will be done for the time to come in fission.

The contributions of "LOHENGRIN" are covered in papers submitted to this conference.

### 3.2 JOSEF

The gas-filled separator JOSEF is operating since 1973. Its specifications are given in table 6. The intensity of the separated fission product beam is increased by a factor 10<sup>3</sup>. The performance exceeds the expectations concerning mass and atomic number resolution <sup>26,27</sup>). Fig. 4a shows a schematic presentation. The characteristic line shapes of the intensity distributions of selected primary  $\gamma$ -transitions are seen from fig. 4b, demonstrating the resolution achieved. Mass and atomic number resolution have been improved compared to former separators by a factor of 4, but still they are by far too small to separate single isotopes admixturefree. The B<sub>p</sub>-values corresponding to the maxima of the intensity distribution plotted versus the mass value are found along straight lines for the different elements according to B<sub>p</sub>/A=f(Z), fig. 4c. The slope of these lines and the distance between adjacent elements depend on the gas filling. A comparison of He- and N<sub>2</sub>-fillings

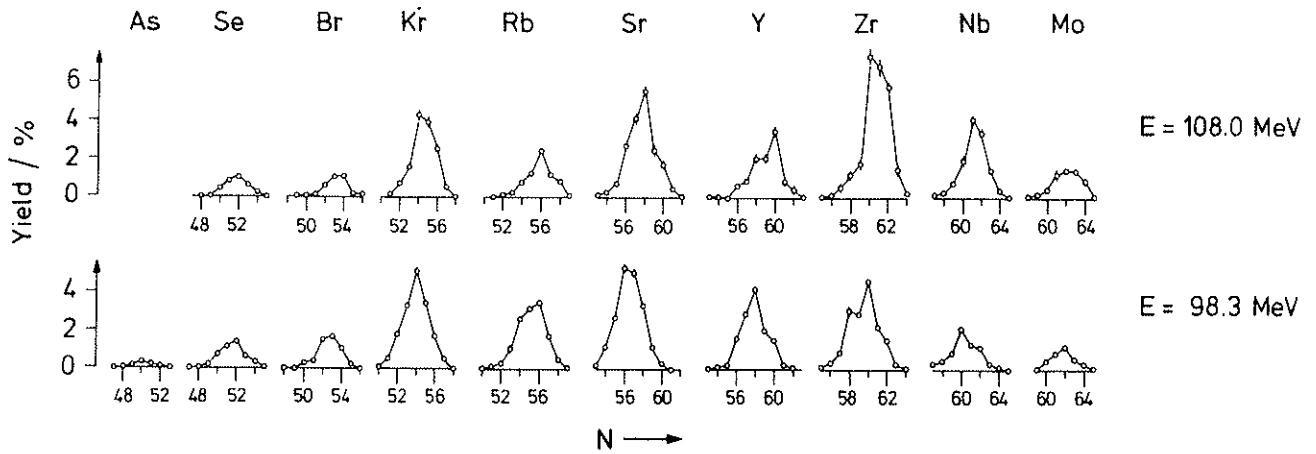


Fig. 3. Absolute independent yields of light fission products from  $^{235}\text{U}(n_{th}, f)$ . The two energies correspond to the average kinetic energy (98.3 MeV) and to high kinetic energies (108 MeV), (H.J. Clerc et al. contr. to this conference).

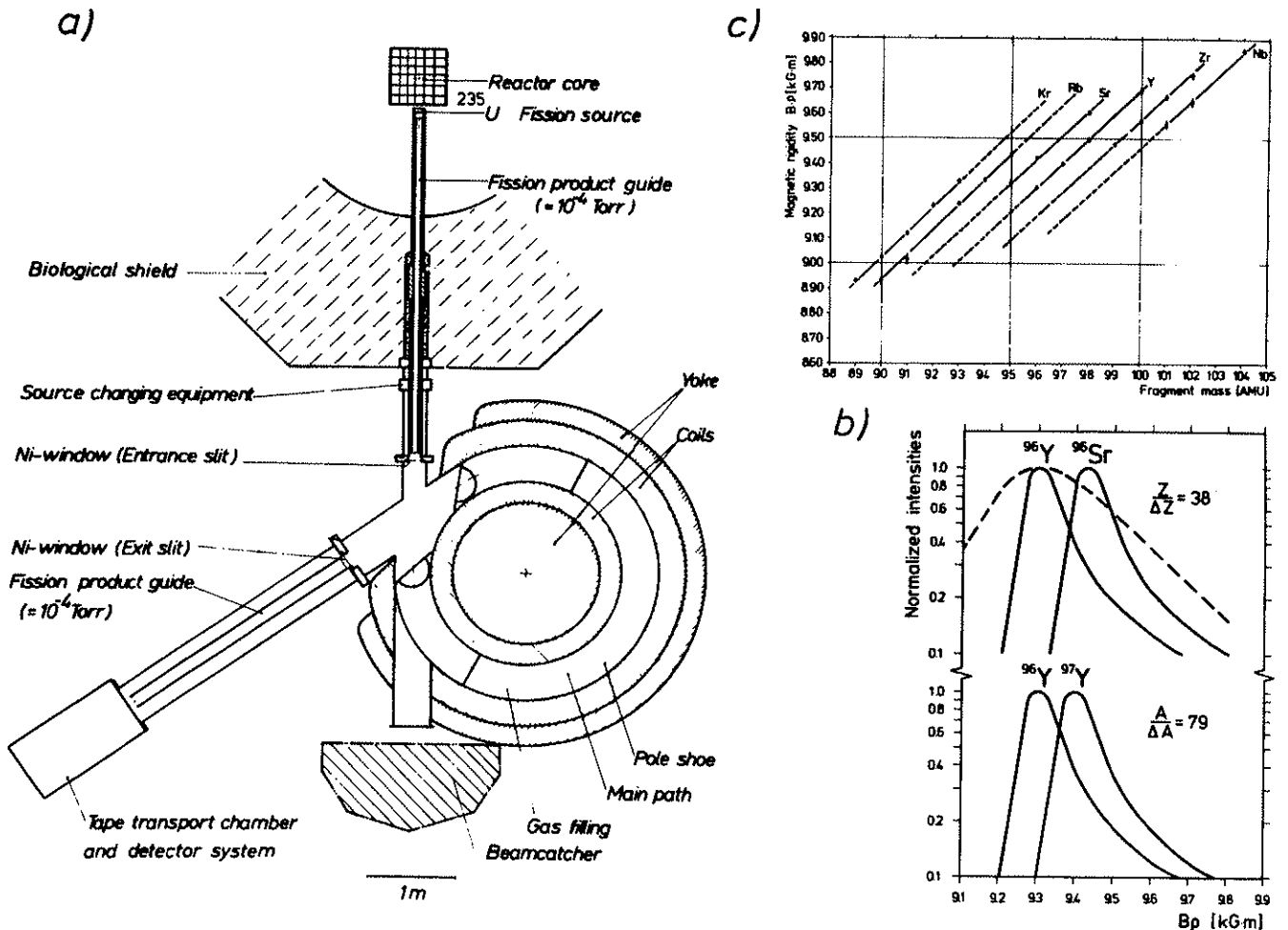


Fig. 4. JOSEF. a) schematic presentation<sup>10)</sup>, b) Intensity distributions of selected isotopes as a function of  $Bp$  demonstrating the mass and atomic number resolution<sup>27)</sup>, c)  $Bp$ -values of primary fission products as a function of mass for He of 4 Torr as a filling<sup>11,27)</sup>.

allows in those few cases where the  $B\rho$ -values of two isotopes coincide an unambiguous isotope identification. The weakest point of older gas-filled magnetic separators, the uncertainty in mass and atomic number assignment has been overcome.

a three-humped intensity distribution for a certain long lived  $\alpha$ -line from element Z already proves the formation of a nucleus (Z+6). The technique may become useful in the identification of new isotopes of heavy elements.

Table 6: Specifications of JOSEF

Target size	35 cm <sup>2</sup>
Target thickness	1 mg/cm <sup>2</sup>
Emittance of guide tube	35x2·10 <sup>-4</sup> cm <sup>2</sup>
Max. magnetic rigidity	1.6 T·m
Main path radius	125 cm
Effective angle of deflection	312°
Radial angle of aperture	6.8°
Axial angle of aperture	2.8°
Solid angle	3.7·10 <sup>-4</sup>
Dispersion	14 m
Magnification	1
Mass Resolution (0.2 Torr N <sub>2</sub> )	79
Atomic Number Resolution (0.2 Torr N <sub>2</sub> )	38
Separated Isotope Rate 2% Fission Yield	3·10 <sup>4</sup> cm <sup>-2</sup> sec <sup>-1</sup>
Total Rate on 200 cm <sup>2</sup>	7·10 <sup>6</sup> sec <sup>-1</sup>

The rates of 7·10<sup>6</sup>/sec for high yield fission products allow all kinds of coincidence studies. Spectroscopy in the A=100 transition region has been performed. Results are presented at this conference.

The intensity distributions of  $\gamma$ -lines from daughter nuclei are records of their origin and genetics. This record can be read analyzing the long lived daughter decays. Fig. 5 gives as an example the intensity distributions of  $\gamma$ -lines in <sup>97</sup>Zr. The very existence of two different types of intensity distributions proves that fission populates states in the mother nucleus, which are not populated by the  $\beta$ -decay of the grandmother. The study of isomers and their population thus becomes a specialty of gas-filled separators. The bookkeeping of genetics may become a useful help in studies of prompt  $\alpha$ - emission and  $\alpha$ -decay chain analysis. For example, the finding of

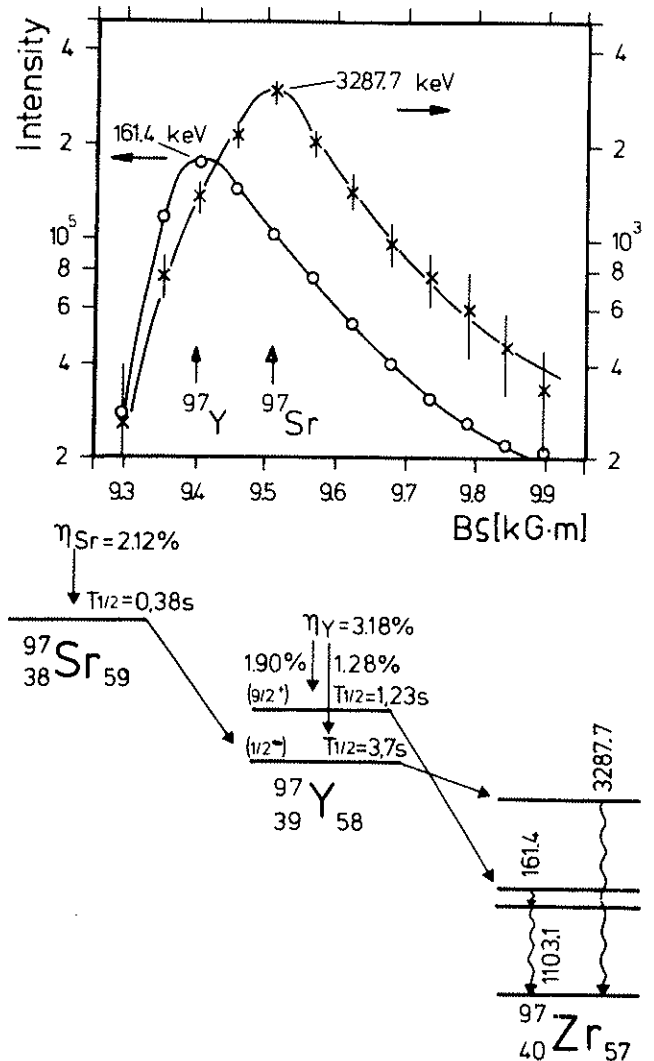


Fig. 5. The decay of A=97 isobars. The  $B\rho$  distribution of <sup>97</sup>Zr  $\gamma$ -transitions show the feeding of  $E_{\gamma} = 161.4$  keV through fission, whereas  $E_{\gamma} = 3287.7$  keV is fed by fission and by  $\beta$ -decay of <sup>97</sup>Sr (27).

### 3.3 SHIP

A collaboration between II. Phys. Institut, University of Gießen and GSI relying on common experiences gained during the construction and operation time of LOHENGRIN accomplished to finish the "SHIP" in time with the availability of beams from UNILAC. The velocity selector SHIP operates since the beginning of 1976. About 40 hours of beam on the target have been given to the experiment for tests and measurements. A list of speci-



fications is found in table 7. The filter is sketched in fig. 6a. The combination of 2 electric and 4 magnetic dipole fields together with 2 quadrupole triplets accepts radially and axially  $3^\circ$ , focusses all ionic charges within an ionic charge window of 20%, and separates out a velocity window of 10%<sup>17,18</sup>). The velocity dispersion necessary to separate projectiles and evaporation residues is maximum in the medium plane of the system. Here the beams are

Table 7: Specifications of the SHIP

Target size	$0.3 \times 1 \text{ cm}^2$
axial and radial entrance aperture	$3^\circ$
exit slit	$3 \times 3 \text{ cm}^2$
axial exit aperture	$3.4^\circ$
radial exit aperture	$2.8^\circ$
distance target-exit	11 m
accepted charge width	20 %
accepted velocity width	10 %
Separated isotope rate	$5 \cdot 10^5 \text{ sec}^{-1}$
Electric fields	
plate distance	15 cm
plate dimension	$50 \times 60 \text{ cm}^2$
max. voltage	800 kV
Dipole magnets	
pole face (3magnets)	$40 \times 50 \text{ cm}^2$
pole face (1magnet)	$40 \times 65 \text{ cm}^2$
gap width	15 cm
max. field strength	0.7 T
Quadrupole magnets	
aperture radius	7,5 cm
iron length	25 cm
max. gradient	9.5 T/m

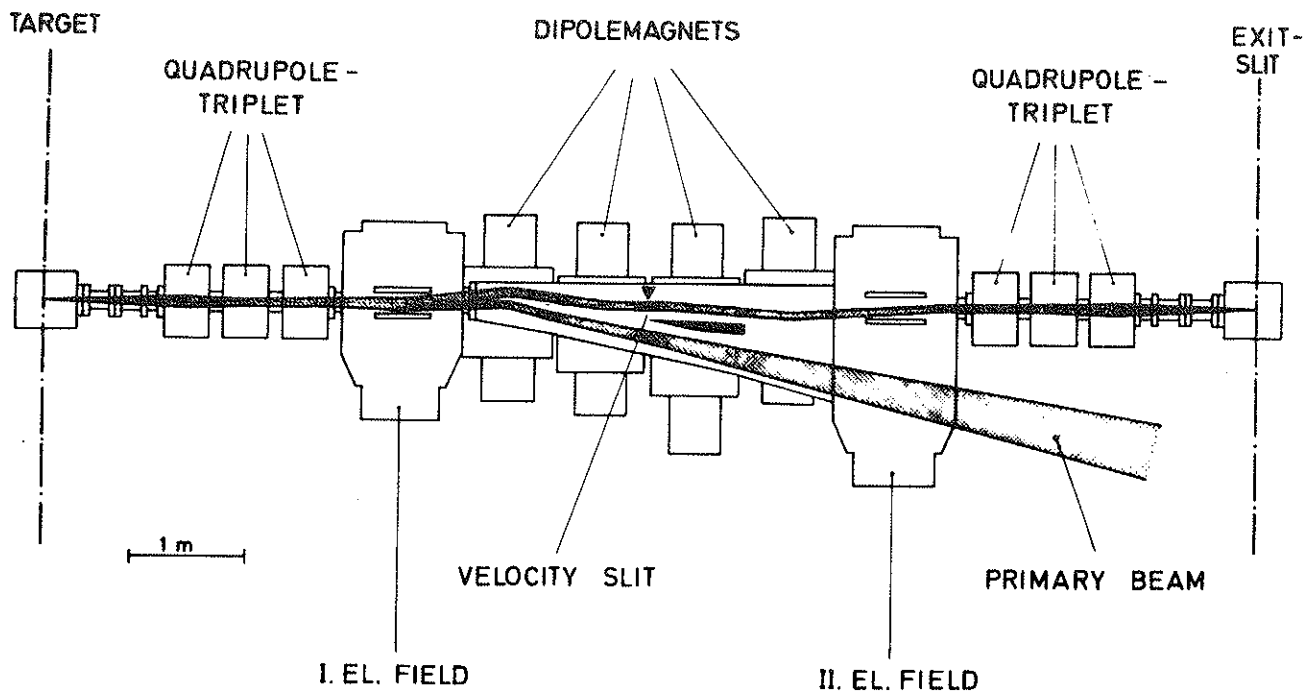
separated. The velocity dispersion is compensated in the second half of the filter, which ionoptically is symmetric to the first half.

The filter has been used with Ar- and Kr-beams of 5.9 MeV/AMU. Targets of  $^{93}\text{Nb}$ ,  $^{144}\text{Sm}$ ,  $^{154}\text{Sm}$ ,  $^{164}\text{Dy}$  have been bombarded in order to produce evaporation residues of atomic numbers between 76 and 84. The  $\alpha$ - and EC-decays of the light isotopes of these elements have been observed. A time-of-flight energy analysis for the (Ar+Sm)- and (Kr+Nb)-reaction products in the velocity window corresponding to the evaporation residues is shown in fig. 6b. The evaporation residues are found in the dominant

single peaks. The background of projectile- and target-like masses is not seen in the Ar case. In the Kr case this background is small, but can be seen at all energies even in the isometric representation. Still the number of particles not falling in the velocity window is small compared to the number of evaporation residues. Projectiles with the primary energy are seen in the Kr bombardment, but were undetectable in the Ar-bombardment. The primary beam is reduced by a factor  $10^{12}$ . The background of projectiles in the velocity window is a fraction of  $10^{-11}$  of the primary beam in the Ar case, a fraction of  $10^{-9}$  in the Kr case.

Fig. 7 shows as an example a set of experiments done during the ( $^{40}\text{Ar} + ^{144}\text{Sm}$ )-irradiation, Fig. 7a gives a surface barrier detector spectrum taken at the exit focus with the velocity window set on the evaporation residues. The spectrum shows a peak of ( $^{40}\text{Ar} + ^{144}\text{Sm}$ )-evaporation residues, a small peak of Ar-projectiles in the velocity window, and the  $\alpha$ -lines of implanted evaporation residues decaying in the detector. The  $10^{14}$  Ar projectiles hitting the target during the measurement give rise to about 500 pulses due to degraded Ar ions in the window. The evaporation residues not decaying by  $\alpha$ -decay decay by e-capture. K $\alpha$  x-ray analysis shows the elemental distribution. Isotopes decaying by e-capture of the elements Pt, Ir, Os and Re must have been produced in the bombardment, as is shown in fig. 7b. An  $\alpha$ -spectrum taken between the beam pulses is shown in fig. 7c. The  $\alpha$ -lines from implanted isotopes show a line width of about 35 keV. They are shifted by about 60 keV to higher energies compared to calibration lines from external sources. The shift is due to the additional energy deposited by the recoils and the absence of energy losses in the detector window. Using known  $\alpha$ -energies given in the literature it was possible to identify as emitters the isotopes  $^{177-179}\text{Hg}$ ,  $^{176-178}\text{Au}$ ,  $^{174-178}\text{Pt}$ <sup>28)</sup>, e.g. the isotope  $^{177}\text{Hg}$  with  $E_\alpha$  6.59 MeV, the lightest Hg-isotope, has been detected in a 10 min. run.

The above techniques combined with cross bombardments and time analysis allow in reasonable measuring times of a few minutes per spectrum to find new  $\alpha$ -emitting isotopes and their half-lives at the border line of stability. Using a second counter as ion counter delayed coincidences will allow to find activities with half-lives as short as microseconds. These half-lives are expected for  $\alpha$ -emitters with  $N > 126$ . Spontaneous fission or any high spin or isomeric state populated in fusion decaying by delayed  $\gamma$ -emission could be detected with the same technique. Detailed studies of the yields of evaporation residues become possible using direct methods to determine mass and atomic numbers. Radiative fusion should, in case it exists, easily be detectable. The system allows to detect low cross section isotopes, as may be found among the heavy or, hopefully, superheavy elements. Cross sections of 0.1 nb in high priority cases still should be measurable.



a)

b)

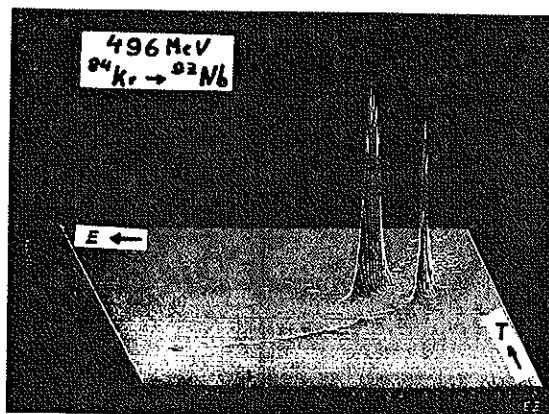
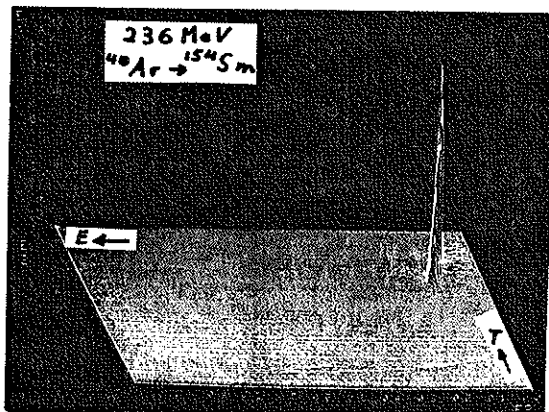


Fig. 6. The SHIP

- a) ion optics of the velocity filter 18)  
 b) TOF-energy measurement of particles in the velocity windows corresponding to (Ar + Sm)- and (Kr + Nb) - evaporation residues.

Electric and magnetic field separators or gas-filled separators behind the SHIP may serve as second stages. LOHENGRIN or JOSEF would be helpful devices. JOSEF would increase the suppression of projectiles without losing more than 50% of the isotope wanted, as its acceptance matches the emittance of the SHIP. Calibrated by known activities an unambiguous identification seems to be possible. LOHENGRIN would allow an unambiguous mass determination. But the rates to be

expected are decreased to values smaller than  $5 \cdot 10^3$ /sec. The decision whether LOHENGRIN, JOSEF or one of their brethren will ride the SHIP depends on the weights put on reaction or isotope production studies. It could be taken after adequate experiences in the operation of the SHIP are available, that is not earlier than the end of this year.

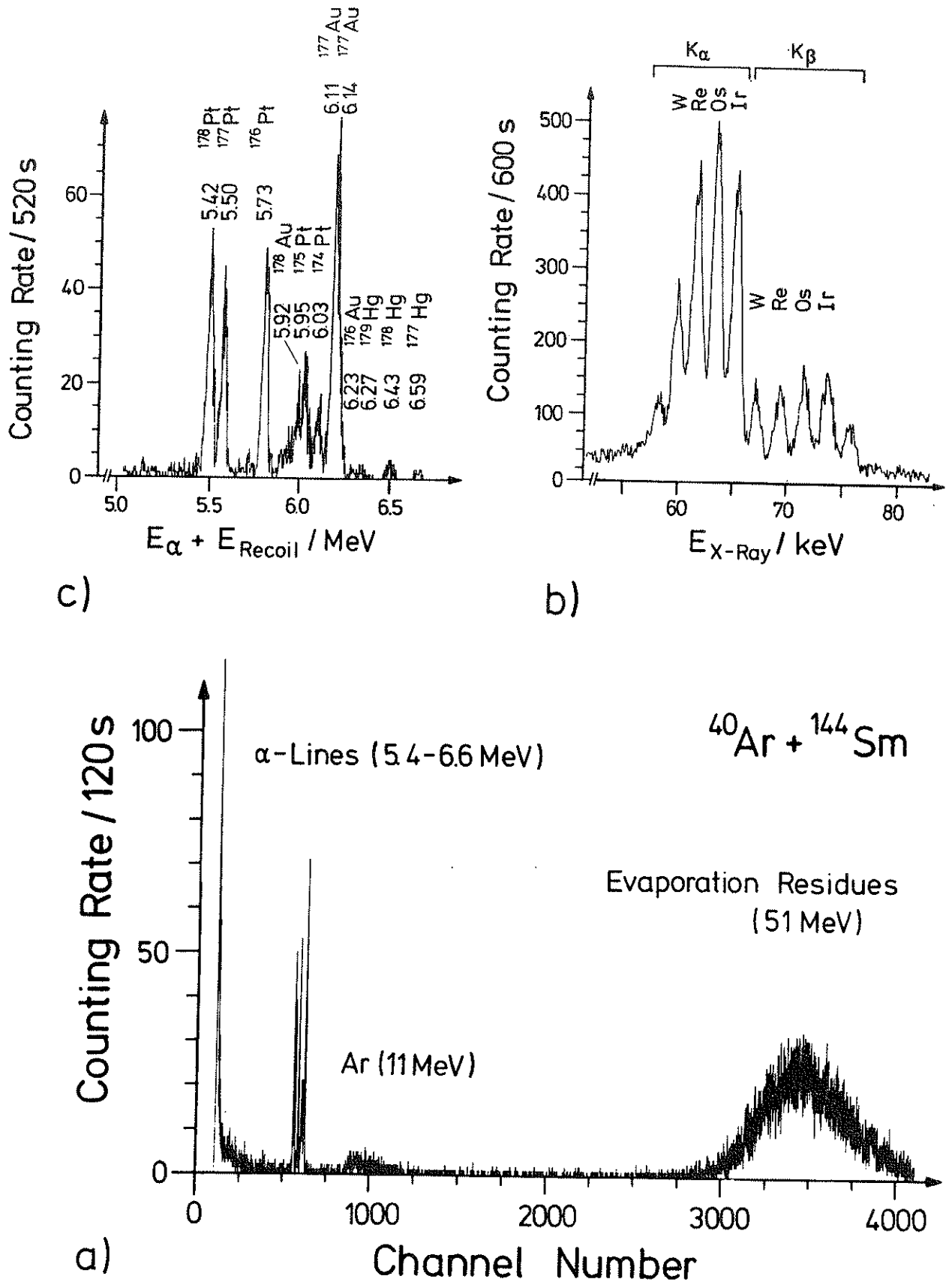


Fig. 7. a) Energy spectrum taken with a surface barrier detector irradiated at the exit focus of SHIP  
 b)  $K_{\alpha}$ -lines from EC-decays of the evaporation residues.  
 c)  $\alpha$ -spectrum of implanted evaporation residues taken between the macropulses of UNILAC.

## References

- 1) H. Ewald, E. Konecny, H. Opower, H. Rösler, Z. f. Naturf. 19a (1964) 194.
- 2) U.A. Arifov, A.D. Belyaev, V.I. Kogan, V.P. Pikul, A.M. Usmandiarov, V.A. Kosilov, N.V. Petrov, Proc. 8th Intern. EMIS Conference on Low Energy Ion Accelerators and mass separators, Skövde (G. Andersson and G. Holmen) (1973) p. 226
- 3) P. Armbruster, H. Ewald, G. Fiebig, E. Konecny, H. Lawin, H. Wollnik, Arkiv för Fysik 36 (1967) 305
- 4) E. Moll, P. Armbruster, H. Ewald, G. Fiebig, H. Lawin, H. Wollnik. Proc. Intern. Conf. on Electromagnetic isotope separators and the techniques of their applications, Marburg, 1970 (eds. H. Wagner and W. Walcher; report BMBW-FB K 70-28, 1970) p. 225.
- 5) E. Moll, H. Schrader, G. Siegert, M. Asghar, J.P. Bocquet, G. Bailleul, J.P. Gautheron, J. Greif, G.J. Crawford, C. Chauvin, H. Ewald, H. Wollnik, P. Armbruster, G. Fiebig, H. Lawin and K. Sistemich, Nucl. Instr. and Methods 123 (1975) 615
- 6) B.L. Cohen, C.B. Fulmer, Nucl. Phys. 6 (1958) 547
- 7) P. Armbruster, Nukleonik 3 (1961) 188
- 8) P. Armbruster, J. Eidens, E. Roeckl, Arkiv för Fysik 36 (1967) 293
- 9) V.A. Karnaukhov, L. Rubinskaya, G.M. Ter Akop'Yan, V. Titov and V.A. Chugreev, report OIYaI P13-4454 (Dubna 1969); see also I. Bacho, D.D. Bogdanov, S. Daroczy, V.A. Karnaukhov, L.A. Petrov, and G.M. Ter Akop'Yan, JINR P 13-4453 (1969)
- 10) H. Lawin, J. Eidens, P. Armbruster, J.W. Grüter, K. Hübenthal, and K. Sistemich, Proc. Int. Conf. on Electromagnetic isotope separators and the techniques of their applications, Marburg 1970 (eds. H. Wagner and W. Walcher; report BMBW-FB K 70-28, 1970) p. 270
- 11) H. Lawin, Thesis (Universität zu Köln 1976),  
H. Lawin, J. Eidens, J.W. Borgs, R. Fabbri, J.W. Grüter, G. Joswig, T.A. Khan, W.D. Lauppe, G. Sadler, H.A. Selić, M. Shaanan, K. Sistemich, to be published Nucl. Instr. and Meth.
- 12) H. Ewald, K. Güttner, P. Hinkel, G. Münzenberg, F. Nickel, H. Wollnik, Proc. 8th Intern. EMIS Conference on Low Energy Ion Accelerators and mass separators, Skövde (G. Andersson and G. Holmen) (1973) p. 220
- 13) E. Kankaleit, F.R. Krueger, B.I. Persson, Nucl. Instr. and Methods 121 (1974) 321
- 14) E. Huenges and H. Vonach, GSI-Report 73-3, p. 26
- 15) S. Skorka, K. Rudolph, J. Hertel, GSI-Report 73-3, p. 1
- 16) D. Evers, R. Glas, W. Hager, P. Konrad, K. Rudolph, S.J. Skorka, Annual Report of the Tandem laboratory TU and LMU, Munique (1975) p. 169
- 17) H. Ewald, K. Güttner, P. Hinckel, G. Münzenberg, W. Faust, F. Nickel, Kerntechnik 16 (1974) 237
- 18) H. Ewald, K. Güttner, G. Münzenberg, P. Armbruster, W. Faust, S. Hofmann, K.H. Schmidt, W. Schneider, K. Valli, Proc. of the 9th EMIS Conf. Kiryat Anavim 1976, to be published
- 19) H. Enge, private communication to R. Bock, GSI
- 20) Proc. of fission information meeting and workshop, ILL-Report 75 A51
- 21) G. Siegert, H. Wollnik, J. Greif, G. Fiedler, M. Asghar, G. Bailleul, J.P. Bocquet, J.P. Gautheron, H. Schrader, E. Ewald, and P. Armbruster, Phys. Lett. 53B (1974) 45
- 22) H.G. Clerc, K.H. Schmidt, H. Wohlfarth, W. Lang, H. Schrader, K.E. Pferdekämper, R. Jungmann, M. Asghar, J.P. Bocquet, and G. Siegert, Nucl. Instr. and Methods 124 (1975) 607
- 23) H.G. Clerc, K.H. Schmidt, H. Wohlfarth, W. Lang, H. Schrader, K.E. Pferdekämper, R. Jungmann, M. Asghar, J.P. Bocquet, G. Siegert, Nucl. Phys. A 247 (1975) 74
- 24) H.G. Clerc, W. Lang, H. Wohlfarth, K.H. Schmidt, H. Schrader, K.E. Pferdekämper, R. Jungmann, Z. Phys. A 274 (1975) 203
- 25) G. Siegert, H. Wollnik, J. Greif, R. Decker, G. Fiedler, B. Pfeiffer, Phys. Rev. C, to be published
- 26) P. Armbruster, J. Eidens, J.W. Grüter, H. Lawin, E. Roeckl, and K. Sistemich, Nucl. Instr. and Meth. 91 (1971) 499
- 27) K. Sistemich, J.W. Grüter, H. Lawin, J. Eidens, R. Fabbri, T.A. Khan, W.D. Lauppe, G. Sadler, H.A. Selić, M. Shaanan, Nucl. Instr. and Meth. 130 (1975) 491
- 28) H. Gauvin, Y. Le Beyec, J. Livet, J.L. Reyss, Ann. Phys. 9.5 (1975) 241.